Gas-Phase Chemistry

Deutsche Ausgabe: DOI: 10.1002/ange.201602604
Internationale Ausgabe: DOI: 10.1002/anie.201602604

UV/Vis Action Spectroscopy and Structures of Tyrosine Peptide Cation Radicals in the Gas Phase

*Emilie Viglino, Christopher J. Shaffer, and František Tureček**

Abstract: *We report the first application of UV/Vis photodissociation action spectroscopy for the structure elucidation of tyrosine peptide cation radicals produced by oxidative intramolecular electron transfer in gas-phase metal complexes. Oxidation of Tyr-Ala-Ala-Ala-Arg (YAAAR) produces Tyr-O radicals by combined electron and proton transfer involving the phenol and carboxyl groups. Oxidation of Ala-Ala-Ala-Tyr-Arg (AAAYR) produces a mixture of cation radicals involving electron abstraction from the Tyr phenol ring and N-terminal amino group in combination with hydrogen-atom transfer from the C_α positions of the peptide backbone.*

The tyrosine residue in proteins and peptides is susceptible to one-electron oxidation, forming aromatic cation radicals and tyrosyl O-radicals as transient reactive intermediates. These biologically important reactions play a role in the functioning of redox enzymes such as galactose oxidase,[1] ribonucleotide reductase,[2] and cytochrome C oxidase[3,4] among others, as reviewed.[5] Tyrosyl radicals in solution and condensed phase have been primarily characterized by electron spin resonance (ESR) spectroscopy and UV/Vis spectroscopy.[6–9] Fast UV/Vis spectroscopy has also been used to characterize tyrosine radicals produced by hydrogen transfer to oxidized tryptophan residues, and a solvent dependence of the absorption maximum has been noted.[10] In contrast to solution and condensed phase studies, transient intermediates that are generated in the gas phase are immune to environmental effects and can be studied as isolated species under strictly unimolecular conditions.[11] Gas-phase tyrosine anion-radicals have been generated by electron photodetachment from peptide molecular dianions and characterized by vacuum UV spectroscopy.[12] Another efficient, and chemically more amenable, method of preparation of gas-phase peptide cation radicals relies on intramolecular one-electron oxidation of a peptide ligand by a transition-metal dication in a ternary complex,[13–15] according to the equation $[Cu^{II}(Ligand)peptide]^{2+\bullet} \rightarrow [Cu^{I}(Ligand)]^{+} + [peptide]^{+\bullet}$. According to their stoichiometry, which is identical to that of the pertinent neutral peptide, peptide cation radicals of this type are called hydrogen-deficient.[16] Tryptophan, a readily oxidizable amino acid, has been characterized as a cation radical in the gas phase by infrared[17] and UV action spectroscopy.[18]

[*] E. Viglino, Dr. C. J. Shaffer, Prof. Dr. F. Tureček
Department of Chemistry, University of Washington
Seattle, WA 98195 (USA)
E-mail: turecek@chem.washington.edu

Supporting information and the ORCID identification number(s) for the author(s) of this article can be found under http://dx.doi.org/10.1002/anie.201602604.

For most part, gas-phase peptide radicals have been studied by collision-induced dissociation (CID) tandem mass spectrometry[13,14] which relies on product analysis but is related only indirectly to the peptide cation radical structure. Clearly, a more direct method of structure elucidation is needed to characterize gas-phase peptide cation radicals formed from metal complexes and resolve the issue of assigning their structure that has persisted for 16 years since the first generation of peptide cation radicals.[19] Here, we report the first study of UV photodissociation (UVPD) action spectroscopy[20] and structure characterization of two tyrosine-containing peptide cation radicals, $YAAAR^{+\bullet}$ and $AAAYR^{+\bullet}$. These representative peptide sequences were selected to provide a well-defined protonation site on the arginine residue and thus to reduce the structural ambiguity to determining the position of the hydrogen-deficient radical site and resolving conformational effects. In addition, these two peptide cation radicals were found to undergo quite different dissociations upon collisional activation and photodissociation, indicating that their radical sites may be different despite being generated by the same electron transfer reaction.

The $YAAAR^{+\bullet}$ and $AAAYR^{+\bullet}$ ions were generated from the respective ternary Cu complexes with 2,2′:6′,2″-terpyridine (tpy) which were formed as doubly charged ions by electrospray ionization.[21,22] CID or laser photodissociation at 355 nm of these doubly charged complexes produced the respective peptide cation radicals at *m*/*z* 550 and their identity was corroborated by accurate mass measurements for the CID-produced ions (Table S1). Peptide cation radicals produced from the ^{63}Cu and ^{65}Cu isotopologues of the $[Cu(tpy)(peptide)]^{2+\bullet}$ complexes showed identical behavior upon CID and UVPD. The photodissociation spectra[23,24] of mass-isolated $YAAAR^{+\bullet}$ and $AAAYR^{+\bullet}$ obtained with a single laser pulse at 355 nm were distinctly different (Figure 1 a,b).

UVPD of $YAAAR^{+\bullet}$ resulted in a dominant elimination of benzoquinone methide (C_7H_6O, 106 Da neutral fragment) from the tyrosine residue. This is a common dissociation of tyrosine-containing hydrogen-deficient peptide cation radicals[13,19] and is also prevalent in the CID spectrum of the $YAAAR^{+\bullet}$ ion (Figure S1a). In contrast, UVPD of $AAAYR^{+\bullet}$ resulted in predominant loss of a hydrogen atom (*m*/*z* 549, Figure 1 b) that was accompanied by a minor elimination of C_3H_4NO from the N-terminal Ala residue (*m*/*z* 480, Figure 1 b). The photo-induced dissociation was dramatically different from CID of $AAAYR^{+\bullet}$ which produced a number of backbone fragment ions, dominated by a major loss of C_3H_4NO from the *N*-terminus. All fragment ion assignments were corroborated by accurate mass measurements (Table S1). The origin of the H atom was investigated with

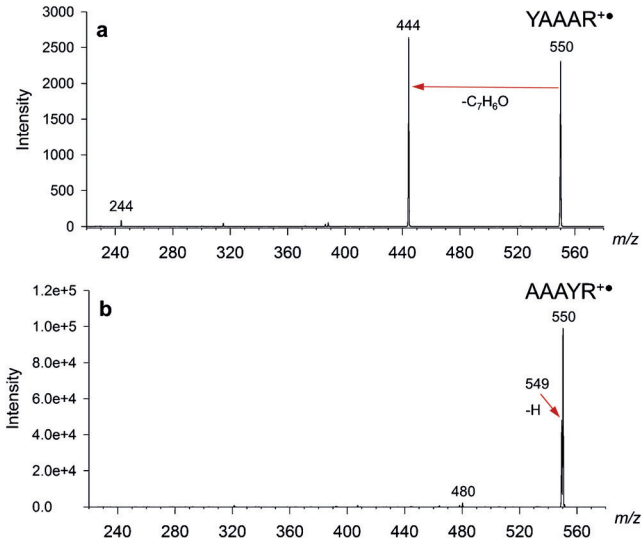

Figure 1. Single-pulse UVPD spectra of a) YAAAR$^{+\bullet}$ and b) AAAYR$^{+\bullet}$ at 355 nm.

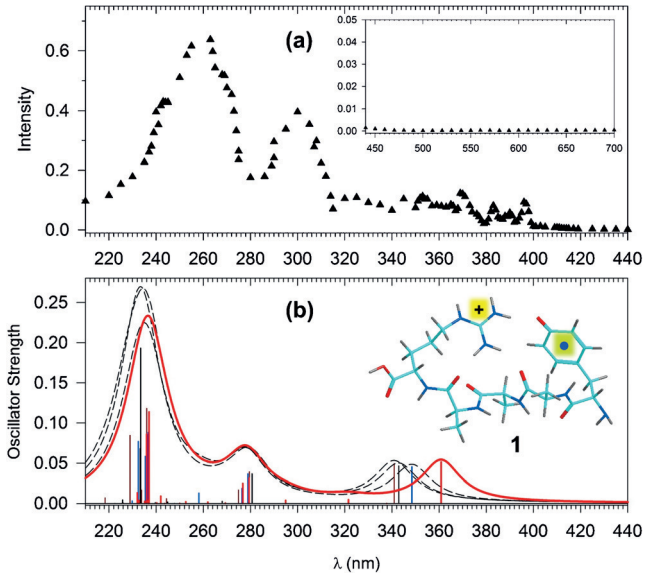

Figure 2. a) Action spectrum of YAAAR$^{+\bullet}$. The trace (▲) shows the wavelength-dependent relative intensity of the major photofragment ion at m/z 444 (loss of C_7H_6O) after single-pulse photodissociation. Inset shows the absorption-free 440–700 nm region. b) Calculated UV/Vis absorption spectra of YAAAR$^{+\bullet}$ conformers **1** (red line) and **2**, **3**, and **4** (dashed lines). The calculated wavelengths (bars) were convoluted with Lorentzian functions at 12 nm fwhm. Inset shows the ωB97X-D optimized structure of **1**. For other conformers see Figure S6 in the Supporting Material.

a lower homologue, AAYR$^{+\bullet}$, which undergoes very similar dissociations upon CID and UVPD as does AAAYR$^{+\bullet}$ (Figure S2a), and in which all the labile protons can be exchanged for deuterium with a high molar conversion (90–93%)[25] to produce d_{11}-AAYR$^{+\bullet}$ (Figure S2b). UVPD of d_{11}-AAYR$^{+\bullet}$ resulted in predominant (>94%) loss of D (Figure S3), indicating that photodissociation selectively targeted the exchangeable hydrogen atoms in the N-H or O–H bonds.

Photodissociation at 355 nm was further studied by pulse-dependent experiments that showed exponential depletion of [YAAAR]$^{+\bullet}$ and [AAAYR]$^{+\bullet}$ ion intensities. This is illustrated by UVPD spectra after 10 laser pulses that show <2% of residual [YAAAR]$^{+\bullet}$ and [AAAYR]$^{+\bullet}$ ions (Figure S4). The photodepletion curve for [YAAAR]$^{+\bullet}$ was fitted with an exponential decay function $I(n) = I(0)e^{-(0.7367n+0.004)} + 0.0035$, where $I(0)$ is the initial [YAAAR]$^{+\bullet}$ ion intensity and n is the number of laser pulses, giving 0.6% root-mean square deviation (rmsd; Figure S5a).

The photodepletion curve for [AAAYR]$^{+\bullet}$ showed a slower decay curve, $I(n) = I(0)e^{-(0.329n+0.113)} + 0.0175$, giving 4.6% rmsd against the experimental data (Figure S5b).

The light absorption properties of YAAAR$^{+\bullet}$ and AAAYR$^{+\bullet}$ were further studied through UV photodissociation action spectra that were measured in the 210–700 nm region. Light absorption was indicated by dissociations forming fragment ions while depleting the precursor cation-radical relative intensity. YAAAR$^{+\bullet}$ showed two major bands with maxima at 260 and 300 nm, and a broad composite band at 340–390 nm. Across this wavelength region the loss of C_7H_6O was the predominant photodissociation channel. No photodissociation was observed above 420 nm (Figure 2a inset). The action spectrum of AAAYR$^{+\bullet}$ was distinctly different, showing bands with maxima at 219, 225 and 246 nm, a broad composite band at 250–310 nm tailing to 380 nm, and another broad absorption band covering the 400–660 nm region (Figure 3). Loss of H was the predominant photodissociation channel across the entire wavelength region

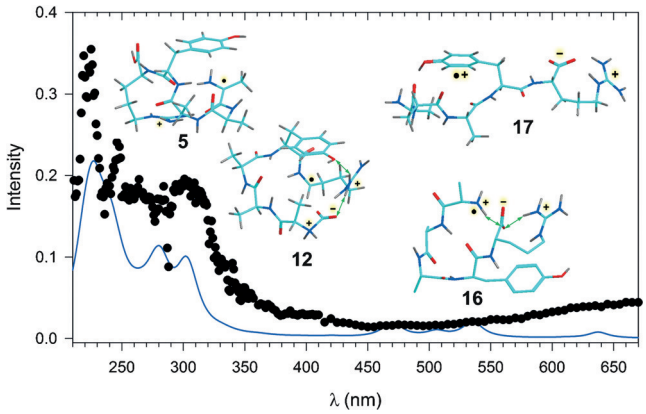

Figure 3. Action spectrum of AAAYR$^{+\bullet}$ (black circles) and combined absorption spectra of **5**, **6**, **12**, **16**, and **17** ion isomers (blue line).

where absorption was observed. The action spectra further indicated that the photodepletion curves at 355 nm were due to only weakly absorbing parts of the spectra, consistent with the slow photodepletion at this wavelength (Figure S5b).

The very different photodissociation and action spectra of YAAAR$^{+\bullet}$ and AAAYR$^{+\bullet}$ strongly indicated that these isomeric peptide cation radicals had different radical chromophore groups. To interpret the action spectra, we performed extensive density functional theory (DFT) calculations of ion structures that were combined with time-dependent DFT (TD-DFT) calculations of electronic excitation energies and oscillator strengths in the cation radicals.

Structures of $YAAAR^{+\bullet}$ were generated in several steps starting with an exhaustive search of the conformational space of arginine-protonated YAAAR ions. Several lowest-energy ions obtained by this procedure were converted to $YAAAR^{+\bullet}$ radicals and fully optimized with B3LYP and ωB97X-D[26] DFT methods, as described in the Supplement (Table S2, Figure S6). Previous benchmarking of excitation energies and transition intensities had identified ωB97X-D as the most reliable TD-DFT method[27] for peptide radical chromophores, which was therefore used to calculate absorption spectra of $YAAAR^{+\bullet}$, as shown for four lowest-energy conformers **1**–**4** (Figure 2b). The calculated spectra show an excellent overall agreement with the experimental action spectrum. The red shift of the major bands in the action spectrum can be in part explained by $v'' \geq 1$ to $v' = 0$ vibronic transitions in thermal ions at the ion trap temperature (310 K), whereas the calculated spectra refer to vertical excitations at 0 K. According to the calculated harmonic frequencies, there are ca. 50 (22%) normal modes in $YAAAR^{+\bullet}$ with frequencies $< 400\ cm^{-1}$ for which statistical thermodynamics analysis[28] predicts $> 20\%$ population of $v'' \geq 1$ states at 310 K.

The two short-wavelength UV bands in Figure 2b are remarkably insensitive to the ion conformation. The 360 nm band for **1** shows a larger spread of excitation energies among **1**–**4** depending on the ion conformation. This can be explained by the electronic nature of this excitation (Figure S7). The major transitions resulting in the 360 nm band involve electron excitation to the semi-occupied aromatic π-orbital at the Tyr residue (MO147). Most of these transitions occur from doubly occupied π-orbitals at backbone amide groups (MO133, 144, 145, 146, Figure S7) and are therefore expected to be sensitive to their position with respect to the Tyr ring, which in turn depends on the peptide ion conformation. Considering the dominant loss of the tyrosine C_7H_6O side chain upon both thermal activation and photoexcitation, as well as the match of the UV-action spectrum with the theoretical electron excitations, we can unequivocally conclude that the $YAAAR^{+\bullet}$ ions formed from the Cu complexes have the structure of Tyr O-radicals.

In contrast to $YAAAR^{+\bullet}$, analysis of the $AAAYR^{+\bullet}$ action spectrum indicated that the ion population consisted of a mixture of isomers. Multiple $AAAYR^{+\bullet}$ structures were generated by exhaustive conformational search followed by DFT geometry optimization. The calculations indicated that one-electron oxidation of the Tyr residue was accompanied by extensive rearrangements and dissociations, yielding only a minority of stable Tyr cation radicals with an electron defect in the aromatic ring. These Tyr cation radicals represented high-energy local potential energy minima that were metastable with respect to exothermic rearrangements or dissociations. Figure S8 shows the representative structures of several types of $AAAYR^{+\bullet}$ isomers (**5**–**18**) which span a broad range of relative energies (Table S3). TD-DFT calculations indicated that none of the several $AAAYR^{+\bullet}$ ion structures alone gave an acceptable match of the theoretical absorption spectrum with the action spectrum. Because of the lack of C_7H_6O elimination from $AAAYR^{+\bullet}$ (Figure 1b), structures **9**–**11** having Tyr O-radical groups (Figure S8) were excluded. Likewise, structures **14** and **15** (Figure S8) having an electron defect in the *N*-terminal amino group were excluded on the basis of their calculated absorption spectra that showed strong absorption bands in the 380–450 nm region which were absent in the action spectrum. In a large number of optimized structures, one-electron oxidation of the carboxyl group resulted in cleavage of the Arg C_α-$COO^\bullet$ bond in the intermittent carboxyl radical, forming ion-molecule complexes of Arg C_α-radicals with CO_2 (e.g., **7** and **8**, Figure S8). Although these complexes had low relative energies, they were only weakly bound ($\Delta H_{diss} < 40\ kJ\,mol^{-1}$) with respect to CO_2 elimination. Since the formation of $AAAYR^{+\bullet}$ by CID of the Cu complexes is not accompanied by CO_2 loss (Figure S9), nor it occurs on UVPD, the CO_2 complexes are unlikely to be present in the population of stable $AAAYR^{+\bullet}$ ions and thus can be excluded. Considering both the spectroscopic data and observed photodissociations, we conclude that the $AAAYR^{+\bullet}$ ions are represented by a mixture of isomers whose combined absorption spectra provide an acceptable agreement with the action spectrum of the ion (Figure 3). The individual spectra of several isomers are shown in Figure S10. Ions **5**, **6**, and **12** (Figure 3) can provide the absorption bands in the 210–350 nm region, but do not have transitions in the visible region. The chromophore in ions **5** and **6** is an Ala-C_α radical group that shows electronic transitions in the 220–380 nm region. Ion **12** and its conformers are Arg-C_α radicals for which we calculate a strong absorption band at 300 nm which is prominent in the action spectrum. We found the *N*-terminal amine cation radicals (**16** and its conformers) and the Tyr aromatic cation radicals (**17** and **18**) as the only chemically compatible structures that had absorption bands in the 450–700 nm region to account for the long-wavelength part of the action spectrum. Ions **5** and **6** belong to the more stable structures (Table S3) in which one-electron oxidation was associated with H_α migration onto the COO group. Ion **12** is also a product of COO^- oxidation, followed by CO_2 migration onto the proximate *N*-terminal amine. Isomer **12** is substantially less stable than **5** and its presence in the oxidized ion population can be only explained by kinetic trapping. Ions **16** and **17**, **18** which result from oxidation of the *N*-terminal amine group and Tyr aromatic ring, respectively, also represent high-energy isomers. In summary, the experimental action spectrum of $AAAYR^{+\bullet}$ is best interpreted as arising from photodissociation of a mixture of cation radical isomers produced by one-electron oxidation of the peptide ligand in the $[Cu(tpy)(AAAYR)]^{2+\bullet}$ complex.

The nature of the observed photodissociations was investigated by analyzing the kinetics of the major reactions of $YAAAR^{+\bullet}$ and $AAAYR^{+\bullet}$. Loss of C_7H_6O from **1** was calculated to be $156\ kJ\,mol^{-1}$ endothermic and required $154\ kJ\,mol^{-1}$ in the transition state for breaking the Tyr C_α-C_β bond, forming the $[^\bullet GAAAR^+ + C_7H_6O]$ complex at $84\ kJ\,mol^{-1}$ relative to **1** (ωB97X-D/6-311++G(2d,p)+ zero-point energies, Table S4). RRKM calculations using these energies and assuming vibronic redistribution of internal energy indicate $< 7\%$ dissociation within the experimental time of 50 ms for **1** having up to $466\ kJ\,mol^{-1}$ internal energy. Considering the mean rovibrational enthalpy of

thermalized **1** (100 kJ mol^{-1} at 310 K) and excitation energy from single photon absorption (337 kJ mol^{-1} at 355 nm), the dissociation is predicted to be slow, leading to < 2 % depletion of **1** (Figure S11a). This contrasts the photodepletion curve of YAAAR$^{+\bullet}$ which shows 55 % dissociation by loss of C_7H_6O in 50 ms following one 355-nm laser pulse (Figure 1 a, Figure S5a). This leads to the conclusion that the photodissociation occurs locally from an excited electronic state involving the Tyr-O radical. The dissociation kinetics under slow-heating conditions of resonant collisional activation can be described by transition-state theory, which gives 90 % dissociation within 50 ms at 700 K (Figure S11b). Such an effective temperature is readily accessible in CID in the ion trap.[29–31]

Similar conclusions can be made regarding the photodissociative loss of an exchangeable H atom from AAAYR$^{+\bullet}$. Calculations of loss of amine and amide H atoms in **5** gave TS energies of > 210 kJ mol^{-1} which were prohibitively high to drive dissociation of an isolated ion in 50 ms. Again, a plausible explanation of the kinetics must consider dissociation proceeding from an excited electronic state but preceding vibronic relaxation of the excitation energy, as described recently for photodissociation of a peptide anion radical.[32] This conclusion is also consistent with the absence of H loss from AAAYR$^{+\bullet}$ upon vibrational activation by collisions in the slow-heating excitation regime (Figure S1b).

The different structures and hence chemistry of YAAAR$^{+\bullet}$ and AAAYR$^{+\bullet}$ are the result of different and sequence-dependent courses of intramolecular electron transfer in the Cu(tpy)(peptide) complexes. The peptide ligand in [Cu(tpy)(YAAAR)]$^{2+\bullet}$ can assume a conformation in which the Tyr side chain is in the vicinity of the Cu-binding COO^- group, forming a hydrogen bond (see the ωB97X-D optimized structures in Scheme 1). Following electron-transfer oxidation, the Tyr cation radical can intramolecularly protonate the COO^- group, forming a Tyr-O radical while weakening the peptide ion bonding to Cu(tpy)$^+$. In contrast, the AAAYR ligand likely adopts several different conformations in the Cu(tpy) complex. Those where Tyr participates in electron transfer presumably lead to the formation of aromatic cation radicals **17** and **18** (Figure S8) whereas oxidized intermediates from other complex conformers are either amine cation radicals (**16**) or carboxyl radicals undergoing rapid stabilization by hydrogen transfer forming the most stable Ala-C_α (**5**) and Arg-C_α (**12**) radical isomers.

In conclusion, UV/Vis photodissociation action spectroscopy allowed us for the first time to establish structures of tyrosine peptide cation radicals formed by intramolecular electron transfer in Cu complexes. The structures point to different modes of peptide ligand oxidation depending on the position of the tyrosine residue in the peptide sequence.

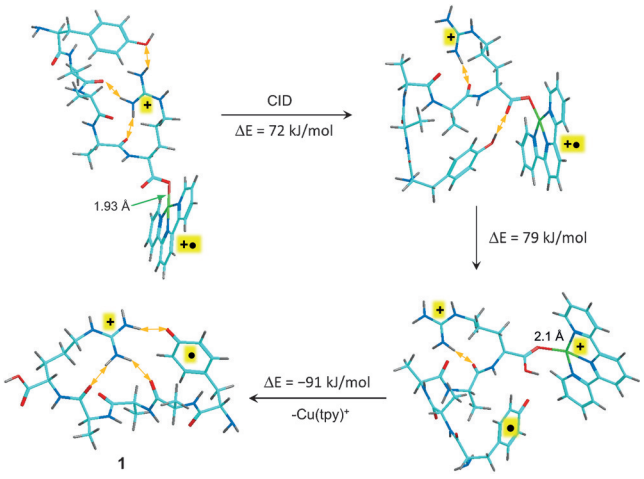

Scheme 1. Conformational transformation in [Cu(tpy)(YAAAR)]$^{2+\bullet}$ followed by intramolecular electron transfer oxidation of the peptide ligand, proton transfer, and dissociation to YAAAR$^{+\bullet}$ (**1**) and [Cu(tpy)]$^+$. The structures and reaction energies are from ωB97X-D/6-311 + + G-(2d,p) calculations. The yellow double-ended arrows indicate major hydrogen bonds.

Experimental Section

All materials were synthesized using standard procedures as described in the Supporting Material section. Photodissociation action spectra were measured for mass-selected peptide cation radicals on a modified LTQ-XL-ETD (ThermoElectron Fisher, San Jose, SA, USA) linear ion trap mass spectrometer equipped with a Nd-YAG laser/OPO laser system. Experimental details and description of calculations are given as Supporting Information.

Acknowledgements

This research was supported by the NSF (grant number CHE-1359810).

Keywords: copper complexes · electron transfer · gas-phase chemistry · peptides · UV/Vis spectroscopy

How to cite: *Angew. Chem. Int. Ed.* **2016**, *55*, 7469–7473
Angew. Chem. **2016**, *128*, 7595–7599

[1] M. M. Whittaker, V. L. DeVito, S. A. Asher, J. W. Whittaker, *J. Biol. Chem.* **1989**, *264*, 7104–7106.
[2] B. M. Sjoberg, P. Reichard, A. Graslund, A. Ehrenberg, *J. Biol. Chem.* **1977**, *252*, 536–541.
[3] M. Voicescu, Y. El Khoury, D. Martel, M. Heinrich, P. Hellwig, *J. Phys. Chem. B* **2009**, *113*, 13429–13436.
[4] G. F. Moore, M. Hambourger, M. Gervaldo, O. G. Poluektov, T. Rajh, D. Gust, T. A. Moore, A. L. Moore, *J. Am. Chem. Soc.* **2008**, *130*, 10466–10467.
[5] J. Stubbe, W. A. van der Donk, *Chem. Rev.* **1998**, *98*, 705–762.
[6] C. Bernini, E. Arezzini, R. Basosi, A. Sinicropi, *J. Phys. Chem. B* **2014**, *118*, 9525–9537.
[7] S. J. Nara, L. Valgimigli, G. F. Pedulli, D. A. Pratt, *J. Am. Chem. Soc.* **2010**, *132*, 863–872.
[8] D. A. Svistunenko, G. A. Jones, *Phys. Chem. Chem. Phys.* **2009**, *11*, 6600–6613.
[9] A. Ivancich, T. A. Mattioli, S. Un, *J. Am. Chem. Soc.* **1999**, *121*, 5743–5753.
[10] M. Faraggi, M. R. DeFelippis, M. H. Klapper, *J. Am. Chem. Soc.* **1989**, *111*, 5141–5145.
[11] F. Tureček, *Top. Curr. Chem.* **2003**, *225*, 77–129.
[12] C. Brunet, A. Claire, R. Antoine, A.-R. Allouche, P. Dugourd, F. Canon, A. Giuliani, L. Nahon, *J. Phys. Chem. A* **2011**, *115*, 8933–8939.
[13] E. Bagheri-Majdi, Y. Ke, G. Orlova, I. K. Chu, A. C. Hopkinson, K. W. M. Siu, *J. Phys. Chem. B* **2004**, *108*, 11170–11181.

[14] C. K. Barlow, S. Wee, W. D. McFadyen, R. A. J. O'Hair, *Dalton Trans.* **2004**, *20*, 3199.
[15] A. C. Hopkinson, *Mass Spectrom. Rev.* **2009**, *28*, 655.
[16] F. Tureček, R. R. Julian, *Chem. Rev.* **2013**, *113*, 6691 – 6733.
[17] A. Piatkivskyi, S. Osburn, K. Jaderberg, J. Grzetic, J. D. Steill, J. Oomens, J. Zhao, J. K.-C. Lau, U. H. Verkerk, A. C. Hopkinson, K. W. M. Siu, V. Ryzhov, *J. Am. Soc. Mass Spectrom.* **2013**, *24*, 513 – 523.
[18] B. Bellina, I. Compagnon, S. Houver, P. Maitre, A.-R. Allouche, R. Antoine, P. Dugourd, *Angew. Chem. Int. Ed.* **2011**, *50*, 11430 – 11432; *Angew. Chem.* **2011**, *123*, 11632 – 11634.
[19] I. K. Chu, C. F. Rodriquez, T. C. Lau, A. C. Hopkinson, K. W. M. Siu, *J. Phys. Chem. B* **2000**, *104*, 3393.
[20] N. C. Polfer, P. Dugourd, *Laser Photodissociation and Spectroscopy of Mass-separated Biomolecular Ions. Lecture Notes in Chemistry*, *Vol. 83*, Springer, Heidelberg, **2013**.
[21] I. K. Chu, C. N. W. Lam, *J. Am. Soc. Mass Spectrom.* **2005**, *16*, 1795 – 1804.
[22] I. K. Chu, C. N. W. Lam, *J. Am. Soc. Mass Spectrom.* **2005**, *16*, 763 – 771.
[23] C. J. Shaffer, A. Marek, R. Pepin, K. Slováková, F. Tureček, *J. Mass Spectrom.* **2015**, *50*, 470 – 475.
[24] H. T. H. Nguyen, C. J. Shaffer, R. Pepin, F. Tureček, *J. Phys. Chem. Lett.* **2015**, *6*, 4722 – 4727.
[25] A. Marek, F. Tureček, *J. Am. Soc. Mass Spectrom.* **2014**, *25*, 778 – 789.
[26] J. D. Chai, M. Head-Gordon, *Phys. Chem. Chem. Phys.* **2008**, *10*, 6615 – 6620.
[27] F. Tureček, *J. Phys. Chem. A* **2015**, *119*, 10101 – 10111.
[28] R. C. Dunbar, *J. Chem. Phys.* **1989**, *90*, 7369 – 7375.
[29] S. A. McLuckey, D. E. Goeringer, *J. Mass Spectrom.* **1997**, *32*, 461 – 474.
[30] F. Ichou, A. Schwarzenberg, D. Lesage, S. Alves, C. Junot, X. Machuron-Mandard, J.-C. Tabet, *J. Mass Spectrom.* **2014**, *49*, 498 – 508.
[31] A. V. Tolmachev, A. N. Vilkov, B. Bogdanov, L. Pasa-Tolic, C. D. Masselon, R. D. Smith, *J. Am. Soc. Mass Spectrom.* **2004**, *15*, 1616 – 1628.
[32] M. A. Halim, M. Girod, L. MacAleese, J. Lemoine, R. Antoine, P. Dugourd, *J. Am. Soc. Mass Spectrom.* **2016**, *27*, 474 – 486.

Received: March 14, 2016
Published online: May 9, 2016

